Supporting Information

Tracking Electrical Fields at the Pt/H_2O Interface during Hydrogen Catalysis

Jaeyune Ryu, Yogesh Surendranath*

Department of Chemistry, Massachusetts Institute of Technology,

Cambridge, Massachusetts 02139, United States

yogi@mit.edu

Index *Page*

Experimental details S3–S5

Figure S1. Ionic strength vs pH plots under varying electrolyte conditions S6

Figure S2. Reaction profiles in high ionic strength electrolytes (pH 0.2 – 5.0) S7

Figure S3. Reaction profiles in high ionic strength electrolytes (pH 6.9 – 8.7) S8

Figure S4. Reaction profiles in low ionic strength electrolytes (pH 2.5 – 10.9) S9

Figure S5. Total conversion rate (k_{obs}) vs pH plots under varying electrolyte conditions S10

Figure S6. Total conversion rate (k_{obs}) and product selectivity as a function of applied potential bias S11

Figure S7. Estimation of error if the Reaction Plane (RP) were beyond the Outer Helmholtz Plane (OHP) S12

References S13

Experimental and Analytical Details

Chemicals and Materials. Sodium perchlorate (99.95%), perchloric acid (99.999%), sodium phosphate dibasic dihydrate (>99%), sodium phosphate monobasic (99.999%), sodium hydroxide (99.99%), *cis-2-butene-1,4-diol* (97%), lithium citrate tribasic tetrahydrate (99.5%), and d^6-dimethyl sulfoxide (DMSO, >99%) were obtained from Sigma Aldrich and used as received. Citric acid anhydrous (99.5%) and ammonium citrate tribasic (>97%) were obtained from Alfa Aesar and used as received. Sodium citrate dihydrate (99%), were obtained from J.T. Baker and used as received. Deuterium oxide (D_2O, >99%) was obtained from Cambridge Isotope Laboratories and used as received. All electrolyte solutions were prepared with reagent grade water (Millipore, 18 MΩ-cm resistivity). Titanium wire and graphite foil were obtained from Alfa Aesar. Pt/C (0.5 mg cm^{-2}) gas diffusion electrodes (GDE) were obtained from the Fuel Cell Store.

Preparation of citrate buffer solutions. 1000 mL batches of 100 mM citrate solution containing 280 mM of Na^+ (pH 6.0) were prepared by dissolving anhydrous citric acid (8 mmol, 1.54 g) and trisodium citrate, dihydrate (92 mmol, 27.1 g) in reagent grade water and adjusting to a total volume of 1000 mL. 1000 mL batches of 100 mM citrate solutions containing 280 mM Li^+ and NH_4^+ (pH 5.8) were prepared by dissolving anhydrous citric acid (8 mmol, 1.54 g) and lithium citrate tribasic tetrahydrate (92 mmol, 26.0 g) and ammonium citrate tribasic (92 mmol, 22.4 g), respectively, in reagent grade water and adjusting to a total volume of 1000 mL. The pH of each solution was adjusted by addition of perchloric acid. For solutions containing 40 mM of Na^+, Li^+, and NH_4^+, the above concentrated solutions were diluted 7-fold with reagent grade water. For solutions containing 8 mM of Na^+, Li^+, and NH_4^+, the above concentrated solutions were diluted 35-fold with reagent grade water. Using the CurTiPot™ software,[1] the ionic strength of each electrolyte was calculated for each pH value and the results are plotted in **Figure S1, square**. We found that the ionic strength for the 280, 40, and 8 mM Na^+ concentration solutions remained roughly constant throughout the pH range (**Figure S1, square**).

Preparation of phosphate buffer solutions. 1000 mL batches of 140 mM phosphate solution containing 280 mM of Na^+ (pH 9.2) were prepared by dissolving dibasic phosphate anhydrous (140 mmol, 19.5 g) in reagent grade water and adjusting to a total volume of 1000 mL. 1000 mL batches of a 280 mM phosphate solution containing 280 mM of Na^+ (pH 4.5) were prepared by dissolving sodium phosphate monobasic (280 mmol, 33.4 g) in reagent grade water and adjusting to a total volume of 1000 mL. The pH of each solution was adjusted by addition of perchloric acid. For solutions containing 40 mM of Na^+, the above concentrated solutions were diluted 7-fold with reagent grade water. For solutions containing 8 mM of Na^+, the above concentrated solutions were diluted 35-fold with reagent grade water. Using the CurTiPot™ software,[1] the ionic strength of each electrolyte was calculated for each pH value and the results are plotted in **Figure S1,**

diamond. We found that the ionic strength for the 280, 40, and 8 mM Na^+ concentration solutions remained roughly constant throughout the pH range (**Figure S1, diamond**).

General reaction conditions. For the reaction of *cis-2-butene-1,4-diol* (1.7 mmol) with hydrogen (1 atm), occurring at open-circuit, a single chamber three electrode cell was used. The cell was comprised of a hanging-strip Pt/C GDE (60%, 0.5 mg cm^{-2}) working electrode (1.5 cm^2 exposed to the electrolyte), a Ag/AgCl (saturated KCl, BASF) or Ag wire reference electrode, and graphite carbon counter electrode in a 20 mL scintillation vial containing a magnetic stir bar (2×5 mm) rotated at 700 rpm. When not used in the experiment, Ag/AgCl electrodes were stored in saturated KCl and were periodically checked relative to pristine reference electrodes to ensure against potential drift. Each electrode in the reactor cell was contacted with a titanium wire that was threaded through a septum-sealed cell cap and connected to a Biologic VSP 16-channel potentiostat. The potentiostat was used to record open circuit potential (OCP) values during each hydrogenation run. The recorded OCP value was converted to the reversible hydrogen electrode (RHE) scale using the following equation, ($E_{RHE} = E_{Ag/AgCl} + 0.198\ V + 0.059V \times pH$). All OCP remained constant at 0 V vs RHE in all cases. Each cell contained 7.0 mL of the desired aqueous electrolyte. H_2 (1 atm) was introduced to the cell through a needle and all electrolyte solutions were pre-saturated with H_2 for 30 min prior to the reaction. Subsequently, 0.1 mL (1.7 mmol) of *cis-2-butene-1,4-diol* was added to the cell and H_2 gas was continuously bubbled through the solution over the course of the reaction. All experiments were performed at ambient temperature (21 ± 1 °C).

Monitoring of reaction profiles at open-circuit potentials (Figure 3 and Figure S2–S5). Using the set up described above, H_2 addition reactions of *cis-2-butene-1,4-diol* were investigated at the OCP in 7.0 mL of the corresponding reaction solution. Following 30 min of pre-saturation with H_2 (1 atm), the working electrode equilibrated to an OCP value of 0.0 V vs RHE in all cases. Subsequently, 0.1 mL (1.7 mmol) of *cis-2-butene-1,4-diol* was injected into the reaction cell and the reaction was allowed to proceed with continuous H_2 bubbling. After 30 and/or 60 min, aliquots (50 μL) of the reaction solutions were taken for ^1H NMR analysis. Each aliquot was added to 0.50 mL of D_2O which served as the NMR solvent. ^1H NMR for each sample was recorded at 400 MHz (Bruker) using added DMSO as an internal standard to quantify the reaction products. Integration relative to the internal standard confirmed that the reaction proceeds cleanly in all cases. Thus, percent conversions were determined by relative integration of NMR resonances corresponding to remnant starting substrate and product. For the data in **Figure 2**, the product fraction ratio was determined by ^1H NMR at 20–30% total conversion of *cis-2-butene-1,4-diol*. We verified that graphite foil, used as a counter electrode, is completely inert towards any conversion of *cis-2-butene-1,4-diol*. In addition, the pH of the reaction solution was measured before and after each reaction and remained unchanged in all cases.

Estimation of error if the Reaction Plane (RP) were beyond the Outer Helmholtz Plane (OHP) (Figure S7). It is possible that RP resides further away from the Pt surface than the OHP (the RP cannot be closer than the OHP, since there is no free charge (solvated proton) inside of the

OHP by definition). If the RP is further away, then the probe reaction would sense the proton in the diffuse double layer (DDL) rather than right at the OHP. We quantified possible errors associated with the disparity between RP and OHP, assuming three possible cases, (1) $x_{RP} = x_{OHP}$ + 0.1 nm, (2) $x_{RP} = x_{OHP}$ + 0.2 nm, and (3) $x_{RP} = x_{OHP}$ + 0.3 nm, where x_{RP} and x_{OHP} refer to the distance between electrode surface to RP and OHP, respectively, and x_{OHP} is arbitrarily set to 0.5 nm (**Figure S7**). Taking our measured electrostatic potential at RP, φ_{RP} (in **Figure 5**, 8 mM) values, we first compute the new values of the electrostatic potential at OHP, φ_{OHP} (**Figure S7-a**) under each of the above distance assumptions. We performed this calculation using the **Eq. (S1)**, which approximately describes the electrostatic potential in the diffuse double layer as a function of the distance from OHP ($x_{RP} - x_{OHP}$):[2]

$$\varphi_{RP} = \varphi_{OHP}\, e^{-\kappa(x_{RP}-x_{OHP})} \text{ or } \varphi_{RP}\, e^{\kappa(x_{RP}-x_{OHP})} = \varphi_{OHP} \quad \textbf{Eq. (S1)}$$

$$\text{where, } \kappa = \sqrt{\frac{2n^o z^2 e^2}{\varepsilon\varepsilon_o kT}} = (3.29\times 10^7)\, C^{*1/2}$$

(C^* is the bulk 1:1 electrolyte concentration in mol/L and κ is given in cm^{-1})

We then took the newly computed φ_{OHP} (**Figure S7-a**) for each condition along with **Eq. (3)** to compute new values of φ_M (**Figure S7-b**). From these computations, we conclude that the possible errors arising from the RP residing in the DDL are not very significant – extension of the RP into the DDL by 0.1 or 0.3 nm leads to small changes in the slope of metal electrostatic potential (**Figure S7-b**) from 58 to 69 mV pH^{-1}, but preserves the overall trend. These small changes lead to corresponding small variation in the estimated E_{PZFC} (**Figure S7-c**) ranging from –0.04 V to –0.06 V and close to ~0.05 V vs SHE value (**Figure 6c**) obtained by assuming that the RP is at the OHP. We also stress that because of the size of the molecule, the alcoholic group (oxygen) that is interacting with the proton cannot be more than ~0.5–0.7 nm from the surface (the aggregate width of a Pt-C, C-C and C-O bond) making the assumption of the RP being 0.8 nm (0.5 nm + 0.3 nm) from the surface is a reasonable upper-bound on the length scale of RP from the surface.

Supporting Figures

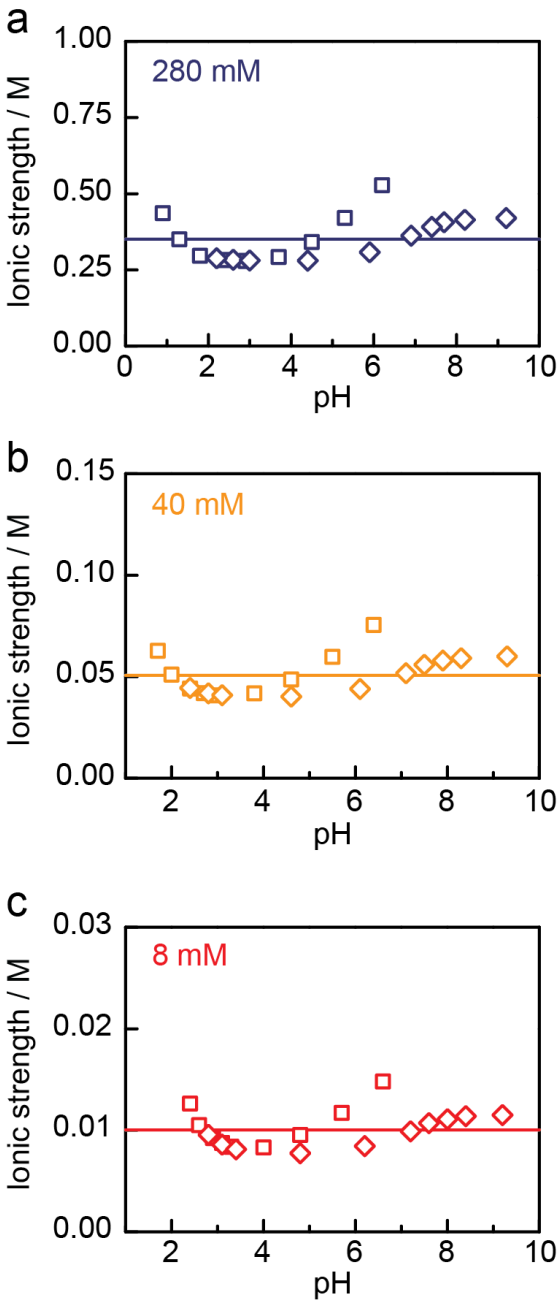

Figure S1. Calculated pH-dependence of total ionic strength for the electrolyte solutions used in this study. Values correspond to (a) 280 mM (blue, I~0.4 M), (b) 40 mM (orange, I~0.05 M), and (c) 8 mM (red, I~0.01 M) of the electrolyte cation ($Na^+/Li^+/NH_4^+$). Square and diamond points correspond to values computed for citrate and phosphate buffers, respectively. The ionic strength values were computed using the CurTiPot™ software[1].

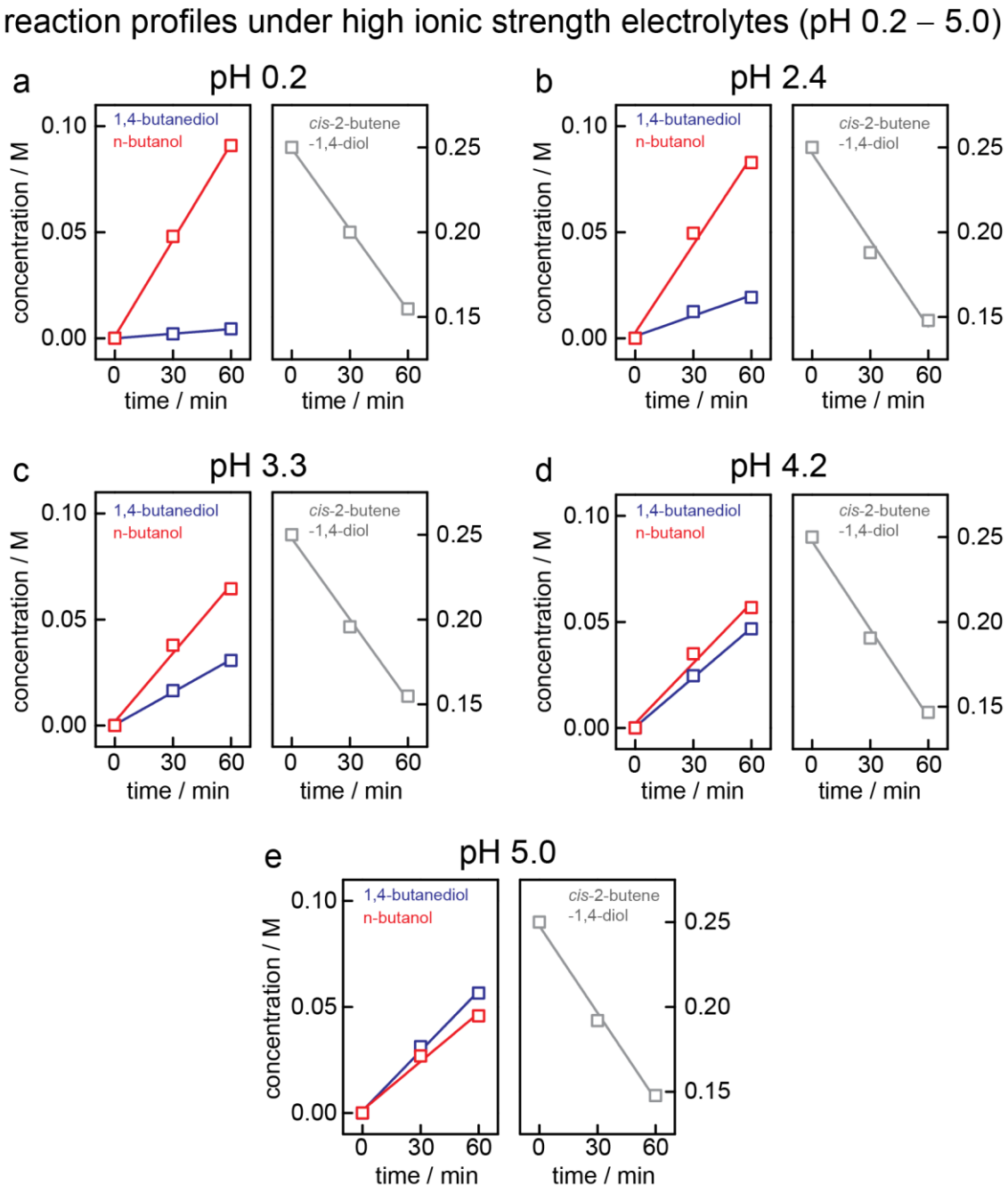

Figure S2. Reaction profiles for production (left) of *n-butanol* (red) and *1,4-butanediol* (blue) as well as consumption (right) of *cis-2-butene-1,4-diol* (grey) recorded under high ionic strength electrolytes, containing 280 mM of Na^+ at pH values of (a) 0.2, (b) 2.4, (c) 3.3, (d) 4.2, and (e) 5.0. Lines represent linear fits to the data.

reaction profiles under high ionic strength electrolytes (pH 6.9 – 8.7)

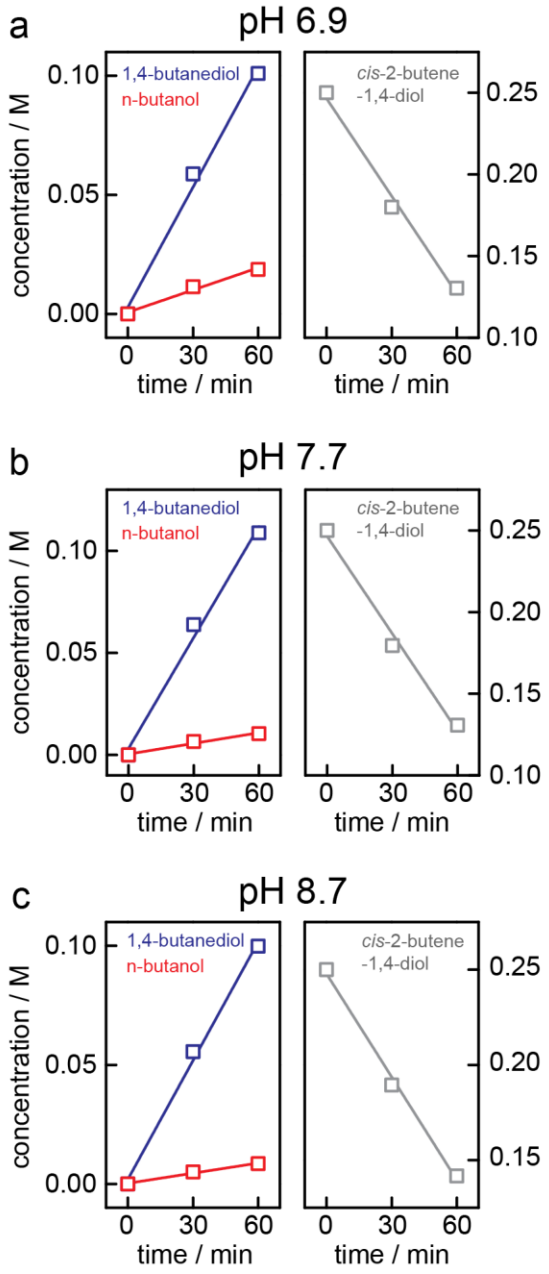

Figure S3. Reaction profiles for production (left) of *n-butanol* (red) and *1,4-butanediol* (blue) as well as consumption (right) of *cis-2-butene-1,4-diol* (grey) recorded under high ionic strength electrolytes, containing 280 mM of Na^+ at pH values of (a) 6.9, (b) 7.7, and (c) 8.7. Lines represent linear fits to the data.

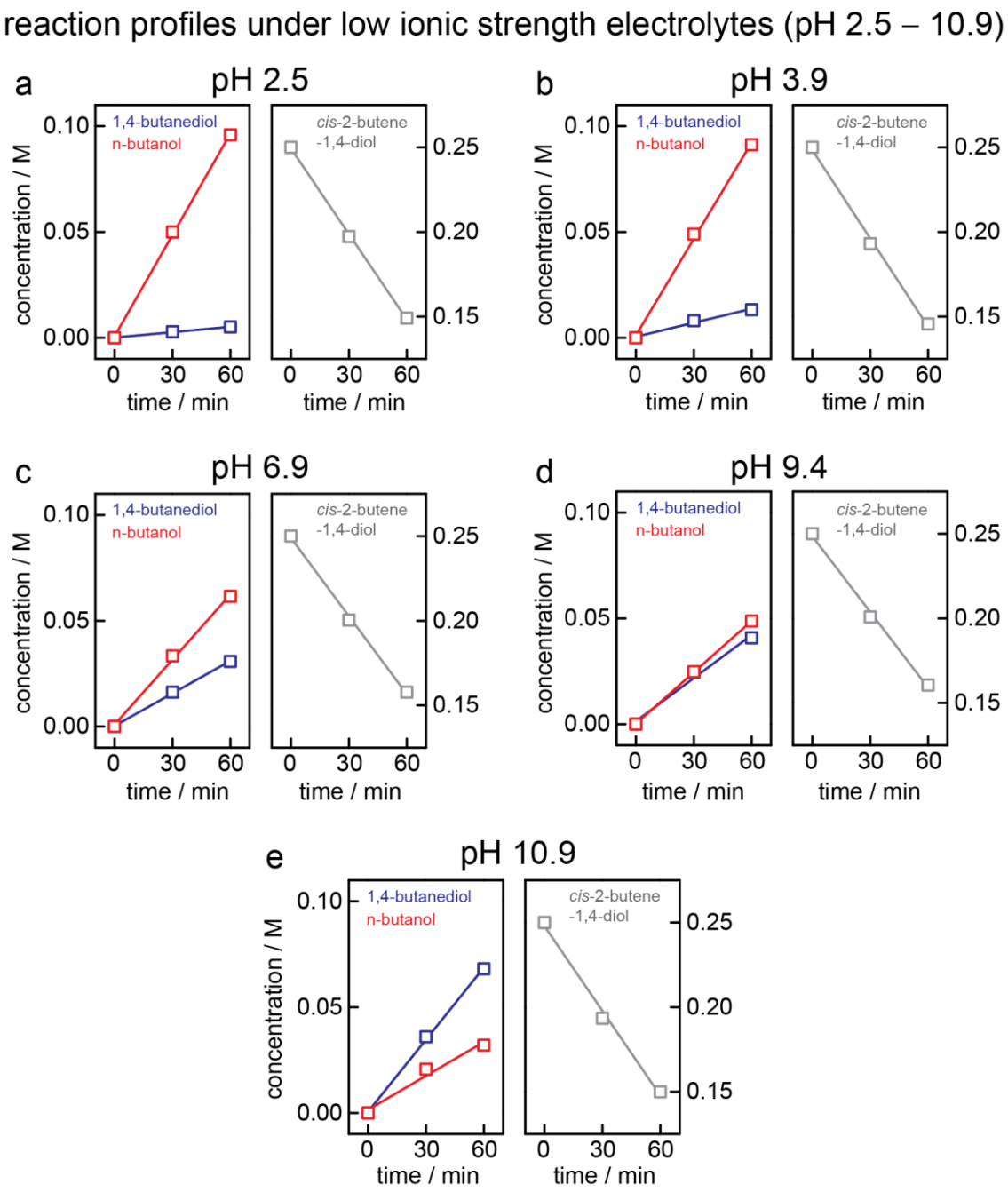

Figure S4. Reaction profiles for production (left) of *n-butanol* (red) and 1,4-butanediol (blue) as well as consumption (right) of *cis-2-butene-1,4-diol* (grey) recorded under low ionic strength electrolytes, containing 8 mM of Na^+ at pH values of (a) 2.5, (b) 3.9, (c) 6.9, (d) 9.4, and (e) 10.9. Lines represent linear fits to the data.

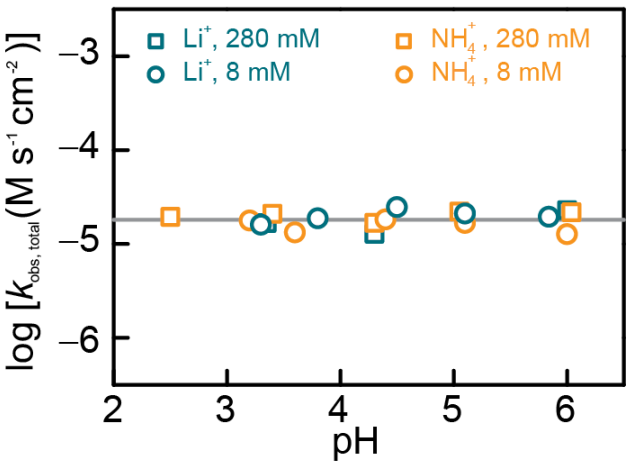

Figure S5. Log k_{obs} versus pH for the rate of total conversion. Squares correspond to data collected with high ionic strength electrolytes, containing 280 mM of Li^+ (green) and NH_4^+ (orange). Circles correspond to data collected with low ionic strength electrolytes, containing 8 mM of Li^+ (green) and NH_4^+ (orange).

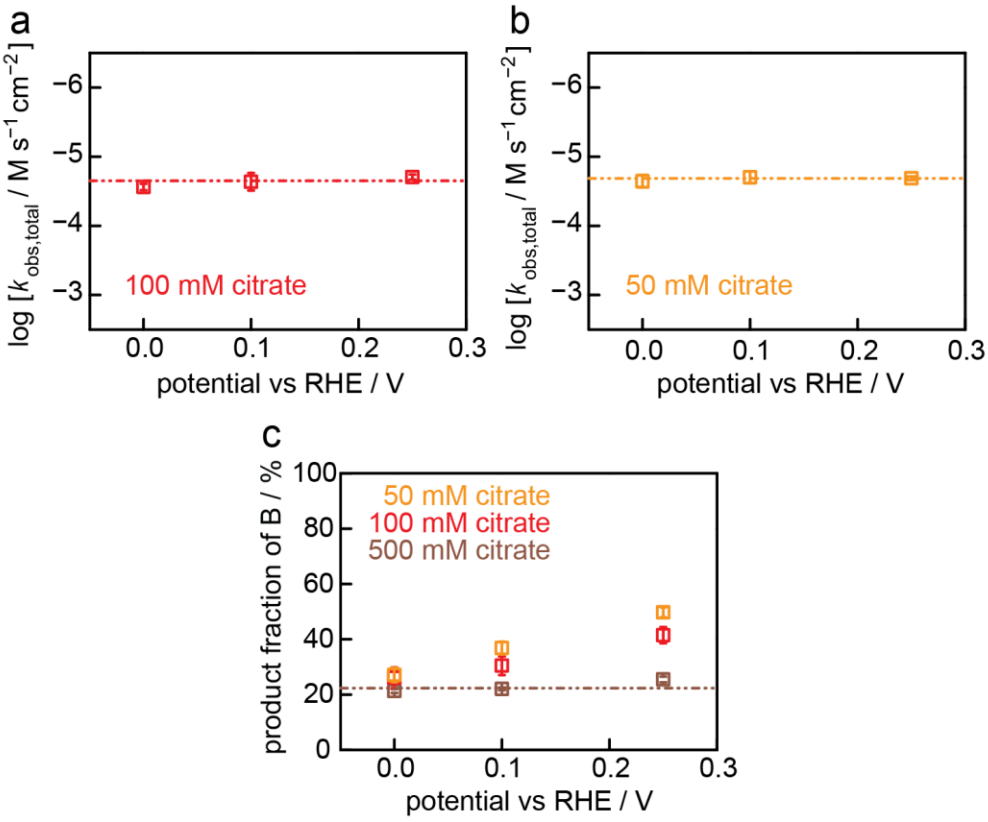

Figure S6. Total conversion rate of *cis-2-butene-1,4-diol* vs applied potential. Data collected in (a) 100 mM citrate / 0.5 M $NaClO_4$, pH 5.8, (b) 50 mM citrate / 0.5 M $NaClO_4$, pH 5.8. (c) Product fraction of *n-butanol*, B (in %), for Pt/C catalyzed H_2 addition to *cis-2-bututene-1,4-diol* as a function of applied potential in the presence of 50 (orange), 100 (red), and 500 (brown) mM citrate with 0.5 M $NaClO_4$ supporting electrolyte, pH 6.0.[3]

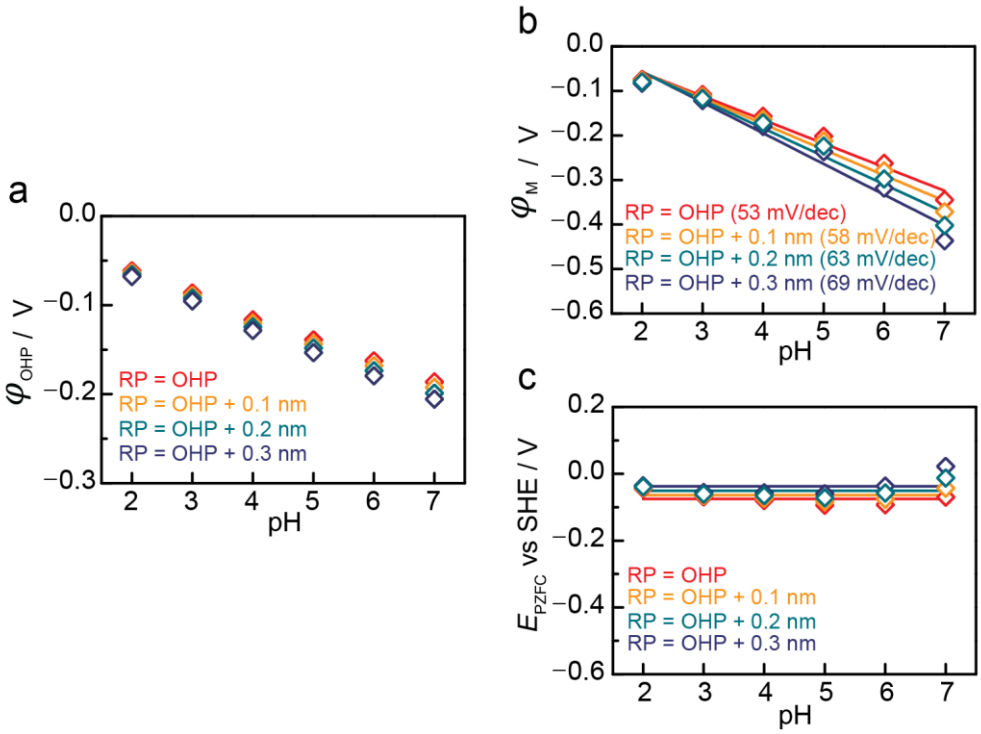

Figure S7. (a) The electrostatic potential at OHP (φ_{OHP}) vs bulk pH, computed using the φ_{RP} in **Figure 5b red** and **Eq. (S1)** upon choosing value of $x_{RP} - x_{OHP}$ of 0.0 (red), 0.1 (orange), 0.2 (green) and 0.3 (blue) nm. (b) The electrostatic potential at the Pt surface (φ_M) vs bulk pH, computed using the φ_{OHP} values obtained in (a) and **Eq. (3)**. The value of x_{OHP} is assumed as 0.5 nm in all cases. (c) The E_{PZFC} values estimated from values in (b).

References

(1) Gutz, I. G. R. CurTiPot pH and Acid-Base Titration 4.2.3 for Excel, http://www.iq.usp.br/gutz/Curtipot_.html.

(2) Bard, A. J.; Larry R. Faulkner. *Electrochemical Methods: Fundamentals and Applications*; Wiley: New York, 2001.

(3) Ryu, J.; Wuttig, A.; Surendranath, Y. *Angew. Chem. Int. Ed*. **2018**, 57, 9300.